

# Evaluation of the Influence of Geometric Parameters on the Accuracy of a Visible Near Infrared (VNIR) Spectroscopy-Based Nitrogen Phosphorus Potassium (NPK) Soil Sensor

Mangeh Elsie Jaja<sup>1,2,3\*</sup>, Valery Nkemeni<sup>1,4</sup>, Pierre Tsafack<sup>1,3</sup>, Pierre Brosselard<sup>4</sup>

<sup>1</sup>Faculty of Engineering and Technology, University of Buea, Buea, Cameroon

<sup>2</sup>National Higher Polytechnic Institute, University of Bamenda, Bambili, Cameroon

<sup>3</sup>Laboratory of Electrical Engineering and Computing, University of Buea, Buea, Cameroon

<sup>4</sup>Laboratoire Ampère (UMR5005), INSA (Institute National des Sciences Appliquées), Lyon, France

Email: \*elsiejajamangeh@yahoo.com, nkemeni.valery@ubuea.cm, tsafack.pierre@ubuea.cm, pierre.brosselard@insa-lyon.fr

**How to cite this paper:** Jaja, M.E., Nkemeni, V., Tsafack, P. and Brosselard, P. (2025) Evaluation of the Influence of Geometric Parameters on the Accuracy of a Visible Near Infrared (VNIR) Spectroscopy-Based Nitrogen Phosphorus Potassium (NPK) Soil Sensor. *Open Journal of Applied Sciences*, 15, 2101-2115.

<https://doi.org/10.4236/ojapps.2025.157138>

**Received:** June 9, 2025

**Accepted:** July 18, 2025

**Published:** July 21, 2025

Copyright © 2025 by author(s) and Scientific Research Publishing Inc.

This work is licensed under the Creative Commons Attribution International License (CC BY 4.0).

<http://creativecommons.org/licenses/by/4.0/>



Open Access

## Abstract

Optimal sensor geometry is crucial for minimizing external light interference, as optical sensing relies on light transmission, which is susceptible to ambient light disruption. This study investigates the influence of geometric parameters on the accuracy of optical sensors used for detecting soil macronutrients. The geometric configuration—specifically the alignment of the photodiode and LEDs was determined using the law of reflection, focusing on parameters such as path length ( $x$ ), angles of incidence ( $\theta_i$ ) and reflection ( $\theta_r$ ), and component distances ( $d_1$ ,  $d_2$ , and  $D$ ). Experimental analysis revealed that the optimal values for  $x$ ,  $D$ , and  $\theta_r$  were 2 cm, 7 cm, and  $60^\circ$ , respectively. At these settings, the sensor achieved minimal error, with RMSE values of 2.1, 0.1, and 1.6 for Nitrogen, Phosphorus, and Potassium concentration measurements, respectively.

## Keywords

Sensors, Optical Sensing Techniques, Visible Near Infrared Spectroscopy, Geometric Parameters

## 1. Introduction

The global population is growing rapidly, resulting in an increase in food demand. As of 2025 (today), the estimated world population stands at approximately 8.2 billion, with previous estimates of 8.1 billion in 2024 [1]. Projections indicate that by 2050, the global population will reach 9.8 billion [1]. Unfortunately, this growth

does not align with an increase in agriculture labour or available farmland due to urbanization [2]. Urban development has led to the continuous loss of agricultural land, through land conversion and non-productive rural activities, such as recreation and hobby farming [3]. This has created a need for advanced technologies in agriculture, giving rise to smart farming, which uses technologies like sensors, actuators, geo-positioning systems and robotics [4] [5]. Smart farming helps enhance productivity and sustainability by monitoring soil parameters, such as pH, temperature, humidity, moisture, and macronutrients (nitrogen (N), phosphorus (P), and potassium (K)). These parameters fluctuate frequently due to environmental factors and human activities making constant monitoring essential for proper plant growth. Sensors play a pivotal role in this monitoring process by providing real-time data necessary to make informed decisions regarding optimized irrigation, fertilization, and crop management.

Maintaining optimal levels of macronutrients (NPK) in soil is essential for proper plant growth. Both excess and insufficient levels can harm plants and the environment. Over-application of NPK can delay maturity, decrease sugar content, and attract pests, while under-application can hinder growth [6]. Using fertilizers cautiously and continuously monitoring nutrient levels can help mitigate these negative effects and environmental pollution.

The sensing technologies used for monitoring soil NPK can be classified into two main categories: optical and electrochemical sensing techniques [7]. Optical sensing which uses light absorption or reflectance properties to estimate nutrient levels is preferred due to its non-destructive nature and cost-effectiveness [8]-[10].

Researchers have made significant advancement in designing optical sensors for the detection of soil macronutrients. Mukherjee and Lasker in [11], developed a Visible Near Infrared (VIS-NIR) based optical sensor for NPK detection, relying on diffused reflectance from soil samples. Lourembam *et al.* in [12], developed an affordable method to monitor soil nitrogen levels by analyzing its unique spectral characteristics. Macabiog *et al.* in [13], developed a near infrared (NIR) spectroscopy sensor, using NIR absorbance variations to assess soil nutrients. Masrie *et al.* [14] designed an optical sensor with light emitting diodes (LED) transmission and photodiode detection systems to classify soil nutrients into low, medium, and high categories. Tasneem *et al.* [15], proposed a colorimetry-based device using LEDs and light depended resistors (LDRs) to measure soil nutrient levels. Mohd. Yusof *et al.* [16] explored soil spectroscopy for monitoring nutrient concentrations through macronutrient absorption peaks. Lavanya *et al.* in [17], developed Internet of Things (IoTs) system to measure soil nutrient levels using reflected light absorbed by an LDR.

Though optical sensing is beneficial for detecting macronutrients in soil, it is crucial to strictly consider the geometrical parameters of the components used in the sensor design. Optimal geometric parameters are necessary to minimize external light interference, as optical sensing relies on light transmission, which ex-

ternal light sources can easily disrupt. Previous studies reviewed above have overlooked this aspect, failing to account for the influence of geometric parameters on the accuracy of an NPK sensor. Therefore, in this study, we investigated the effect of geometric parameters on the accuracy of optical sensor for the detection of soil macronutrients. The key contributions of this study are:

- Investigation the effect of geometric parameters on the accuracy of optical sensors for detecting soil macronutrients (NPK);
- Determination optimal geometric parameters that enhance sensor accuracy and minimize external light interface;
- Validation of sensor performance by using soil samples with chemically verified macronutrient concentration to investigate the impact of geometric parameter variation.

The remainder of this article is organized as follows: Section 2 describes the adopted methodology, Section 3 discusses the results obtained, and Section 4 concludes the paper and offers recommendations for future research.

## 2. Materials and Methods

### 2.1. Proposed System Block Diagram

The block diagram of the experimental setup in the laboratory is presented in **Figure 1**. It consists of four units: the power unit, sensing unit, processing unit, and display unit. The power unit includes a direct current power supply, specifically the GWINSTEK GPS-4303C model, which is crucial for powering other essential system elements. The sensing unit comprises an optical sensor, detailed in the block diagram in **Figure 2**. As shown, the sensor is made up of two sub-units: the transmission and detection units. The transmission unit contains LEDs,

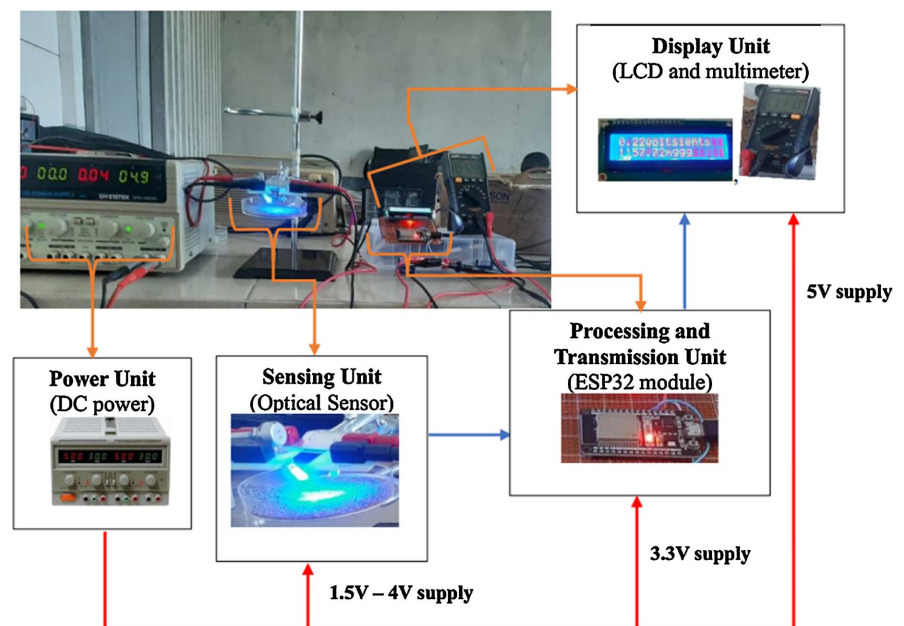


**Figure 1.** Experimental setup block diagram.

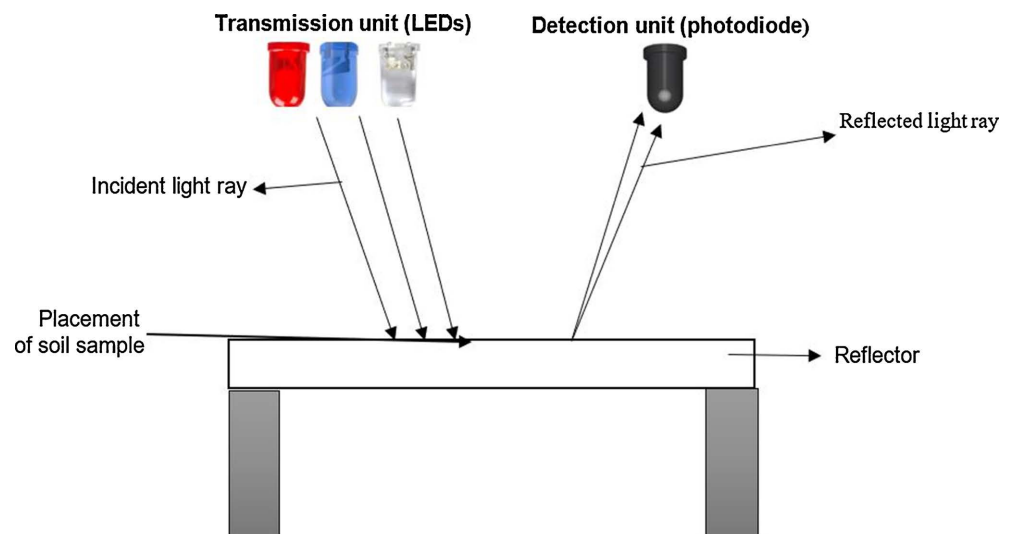


**Figure 2.** Optical sensor block diagram.

while the detection unit includes a photodiode. Specifically, the LEDs used are infrared, red, and blue, which detect the concentrations of Nitrogen, Phosphorus, and Potassium, respectively, due to their corresponding optical features (same absorption wavelengths) as specified in **Table 1**. These LEDs emit visible and infrared optical radiation to experimental samples. The photodiode in the detection unit absorbs light reflected from the experimental samples, producing an output voltage proportional to the reflected light. To minimize the impact of ambient-light interference, all experiments were conducted inside a dark, enclosed box specifically designed to eliminate external light sources. Additionally, to ensure accurate sensor readings, each measurement was performed three times under varying environmental conditions, and the average of these replicates was used in the analysis.

**Table 1.** Optical Characteristics of Macronutrients and corresponding optical light source.

Soil Sample	Optimum Absorption wavelength (nm)	Corresponding Optical Light source (LED)	Wavelength of light source (nm)	Model of Optical Light source	References
Nitrogen (N)	850	Infrared	800 - 980	TSHF5210	
Phosphorus (P)	620 - 630	Red	620 - 750	L-57IID	[11] [13] [14]
Potassium (K)	460 - 470	Blue	450 - 495	SFH 203 P	

The processing unit, primarily consisting of an ESP32 microcontroller, processes data from the sensor (reflected voltage) using sensor's models incorporated into the program codes loaded onto the microcontroller. The models for determining the concentrations of Nitrogen, Phosphorus, and Potassium are specified in Equations (1)-(3), respectively. These models derived from calibration experi-

ments conducted on multiple experimental samples with varying NPK concentrations. The flowchart diagram for the program code is shown in **Figure 3**. As shown in the flowchart, the initial step of the program involves receiving an input signal from the sensor. These signals correspond to different optical radiation, as detailed in **Table 1**. When infrared radiation is received, the model in Equation (1) is used

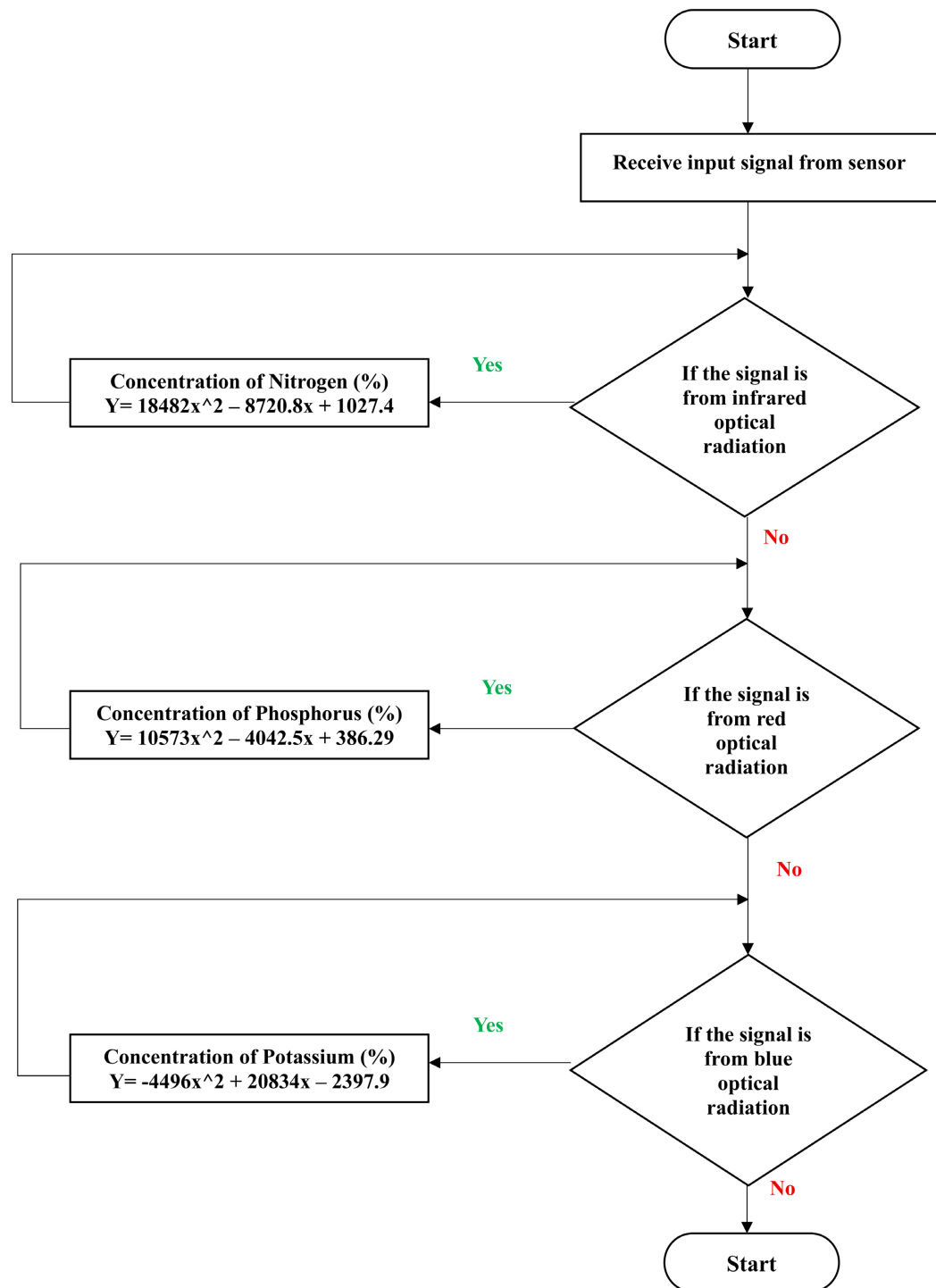


**Figure 3.** Flow chart diagram of program code.

to determine the concentration of N in soil. If the detected optical radiations are red and blue, the models specified in Equations (2) and (3) are used to calculate the concentrations of P and K, respectively. The display unit is made up of an LCD 16 × 2, whose main purpose is to display results from the processing unit, specifically the concentration of macronutrients.

$$y = 18482x^2 - 8720.8x + 1027.4 \tag{1}$$

$$y = 10573x^2 - 4042.5x + 386.29 \tag{2}$$

$$y = -4496x^2 + 20834x - 2397.9 \tag{3}$$

where  $y$  is the concentration of macronutrient (N, P, or K) in percentage (%), and  $x$  is the reflected voltage in volts

### 2.2. Sensor Geometric Parameters

One of the main factors to consider when determining the geometric parameters of optical sensors is the alignment of the different elements constituting the sensor. Since optical sensing involves the transmission of sensed signals in the form of light rays, improper alignment of the sensor elements can lead to significant external light interference [18]. By considering the alignment of sensor elements as key factors in determining the sensor’s geometric parameters, the law of reflection, which states that the angle of reflection equals the angle of incidence, can be used to determine the specific geometric parameters.

These specific parameters include optimal path length ( $x$ ), angle of incidence ( $\theta_i$ ) and angle of reflection ( $\theta_r$ ), and distances between various components ( $d_1$ ,  $d_2$ , and  $D$ ). **Figure 4** provides an illustrative diagram of our sensor with labelled geometric parameters. The  $\theta_i$  was systematically varied within the range  $0^\circ < \theta_i < 90^\circ$ . At  $0^\circ$ , the LED points directly at the photodiode, resulting in minimal reflection, which makes accurate measurements challenging. Similarly, at  $90^\circ$ , the LED points directly at the reflector (sample plate), and the photodiode aligns with the

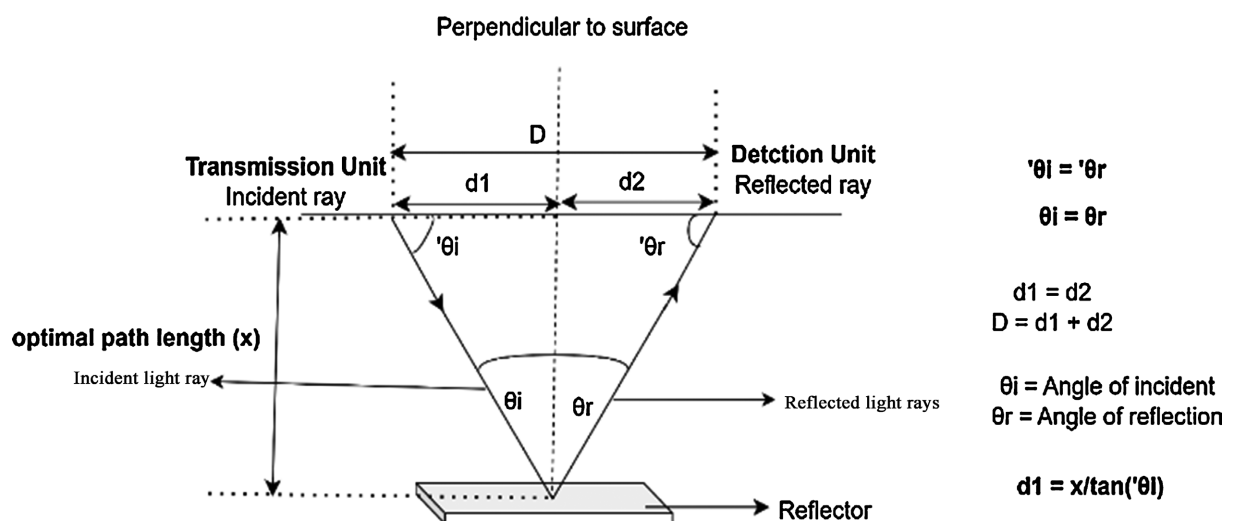


**Figure 4.** Sensor geometric parameters.

reflector, minimizing reflected light detection due to the incident light reflecting along its original path. Therefore, angles of  $0^\circ$  and  $90^\circ$  were avoided. For each angle ( $30^\circ$ ,  $45^\circ$ ,  $60^\circ$ ,  $75^\circ$ ) the corresponding  $x$ ,  $d1$ ,  $d2$ , and  $D$  were determined, as detailed in **Table 2**.

**Table 2.** Detailed variation of geometric parameters.

$\theta_i$	$x$	$d2 = d1$ (cm)	$D = d1 + d2$ (cm)
$30^\circ$	10	17.3	34.6
	8	13.9	27.8
	6	10.4	20.8
	4	6.9	13.8
	2	3.5	7.0
$45^\circ$	10	10.0	20.0
	8	8.0	16.0
	6	6.0	12.0
	4	4.0	8.0
	2	2.0	4.0
$60^\circ$	10	5.8	11.6
	8	4.6	9.2
	6	3.5	7.0
	4	2.3	4.6
	2	1.2	2.4
$75^\circ$	10	2.7	5.4
	8	2.1	4.2
	6	1.6	3.2
	4	1.1	2.2
	2	0.5	1.0

### 2.3. Experimental Sample

The sample used in this experimental procedure was composed of NPK fertilizer and black soil, as illustrated in **Figure 5**. Initially, the experimental sample was air-dried to remove moisture content and then pulverized into a fine powder using a blender. Afterward, the powdered sample was sifted through a sieve to eliminate any sizable particles that might disrupt measurements. Finally, the sample was chemically analysed to determine the exact concentrations (also known as reference concentrations) of Nitrogen, Phosphorus and Potassium as detailed in **Table 3**. Nitrogen analysis involved combusting the analytical samples at  $10,500^\circ\text{C}$  in a helium and oxygen atmosphere. The nitrogen content was converted into

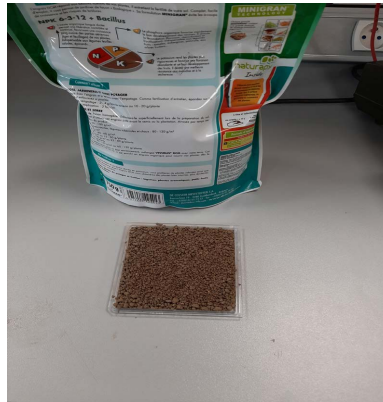


**Figure 5.** A picture of experimental sample.

**Table 3.** Concentration of experimental sample from chemical analysis.

Composition of Experimental Sample	Reference Concentration of Macronutrient (%)		
	N	P	K
Mixture of NPK fertilizer and black soil	4.1	0.9	4.6

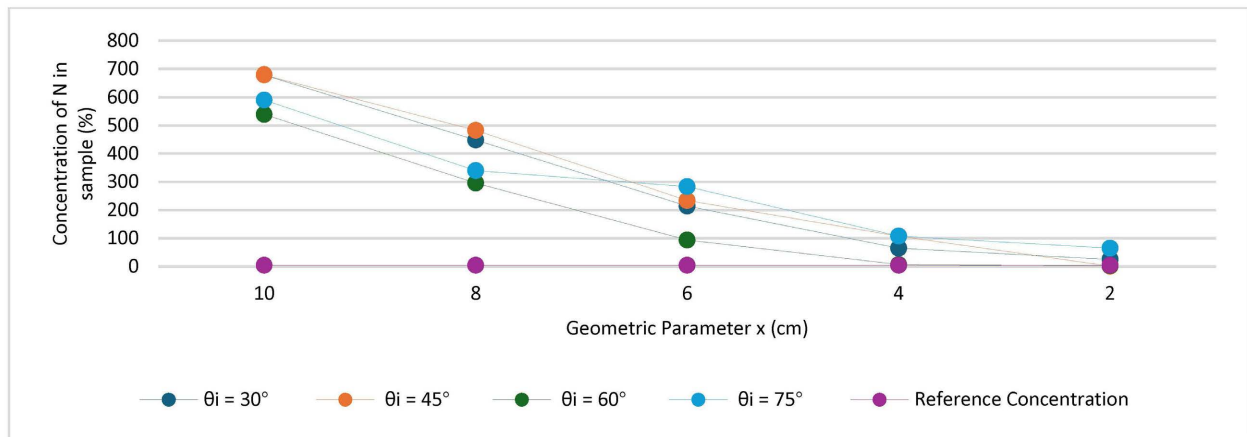
various nitrogen oxides, which were subsequently reduced to molecular nitrogen. Quantification of nitrogen was performed using a thermal conductivity detector. For phosphorus and potassium analysis, Laser-Induced Breakdown Spectroscopy (LIBS) was employed, utilizing the reference material “Monta CRM2710 floor”. LIBS is a rapid and cost-effective technique for analyzing phosphorus and potassium in fertilizers. It works by focusing a laser onto the sample’s surface to create plasma, which is then analyzed to determine the elemental composition. These experiments were conducted at the ISA (Institute of Analytical Sciences) UMR5280, Université Claude Bernard Lyon 1.

### 3. Results and Discussion

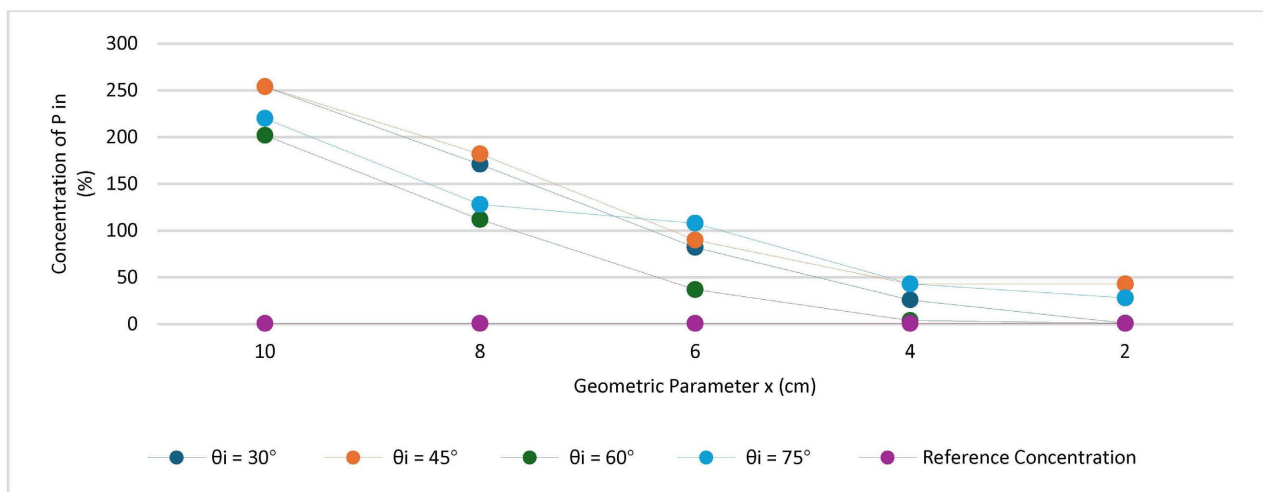
In this section we present and discuss the results obtained from laboratory experiments. Firstly, we examine the effect of geometric parameters on the accuracy of the sensor. Subsequently, we determine the optimal geometric parameters for accurate detection of NPK. Finally, we discuss the influence of these optimal geometric parameters on sensor accuracy and mitigation of external interference.

#### 3.1. The Effect of Geometric Parameters on the Accuracy of the Optimal Sensor

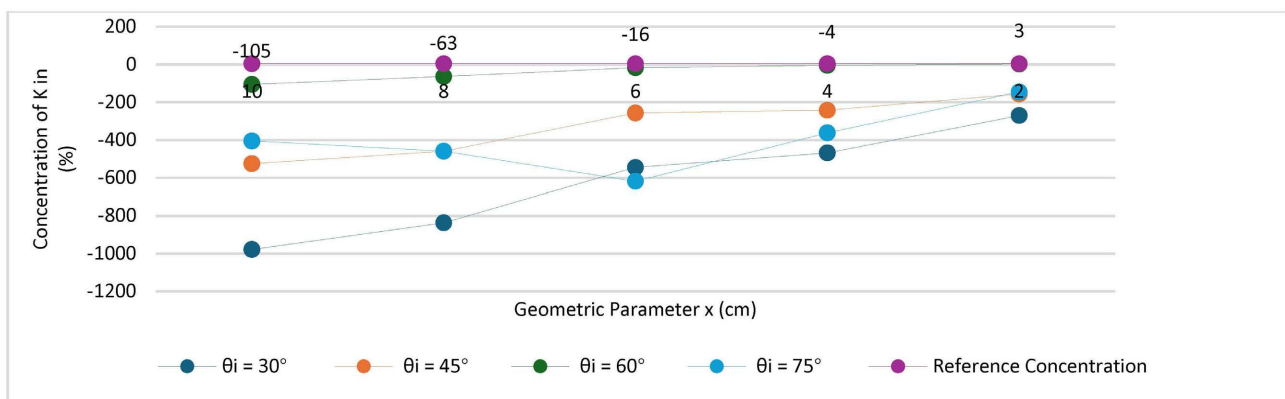
Geometric parameters were varied (as specified in **Table 2**) and their effects on detected soil macronutrients concentration were evaluated. **Figure 6** displays how the measured concentration of NPK varied with changes in the optical path length ( $x$ ) and incidence angle ( $\theta$ ). Results gotten showed that these geometric parameters significantly impact measurement accuracy and sensor reliability. The variation in these parameters influences how external light interacted with the sensor,



(a)



(b)



(c)

**Figure 6.** The variation in concentration of macronutrients in response to changes in Geometric Parameter x (a) Nitrogen (N), (b) Phosphorus (P), (c) Potassium (K).

hence affecting the signal quality and measurement precision of the sensor. Therefore, understanding these effects or change in variations is crucial for optimizing the sensor design, hence ensuring that macronutrients are detected accurately and

efficiently in agricultural farmlands.

For all optical radiation, we noticed significant changes in the concentration of macronutrients (NPK) to changes in optical path length and angle of incidence. As the optical path length increased, the detected macronutrient concentration deviated from the reference concentration. This deviation is mainly due to increased light attenuation along extended optical paths, which leads to signal degradation, hence reduce accuracy. Longer optical paths amplify scattering effects, decreasing sensitivity and complicating nutrient quantification (Li *et al.* [19] and Alem *et al.* [20]). Masrie *et al.* [14] and Yusof *et al.* [16] further emphasized the negative impact of extended optical paths, highlighting that excessive attenuation reduces the ability of the sensors to detect soil nutrients effectively.

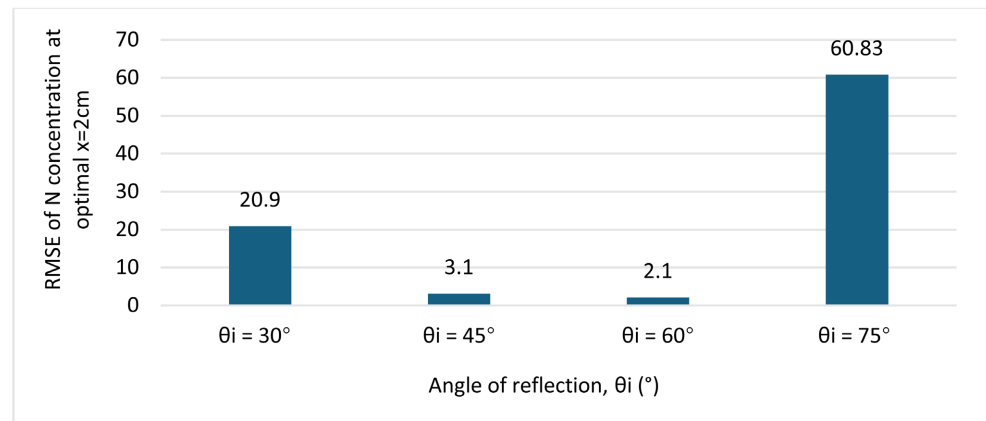
The angle of incidence also exhibited a significant influence on sensor accuracy. Increase in angle of incidence led to greater reflection losses, decreasing the amount of transmitted light that reached the detector. This observation supports the results presented by Ahmed *et al.* [21] and Liu *et al.* [22], which demonstrated that optimizing angle of incidence enhances the measurement stability by balancing absorbed and reflected light intensity with light transmission efficiency. These findings indicate that geometric parameter optimization is vital for improving sensor performance and ensuring reliable macronutrient detection in precision agriculture.

### 3.2. Determination of Optimal Geometric Parameters

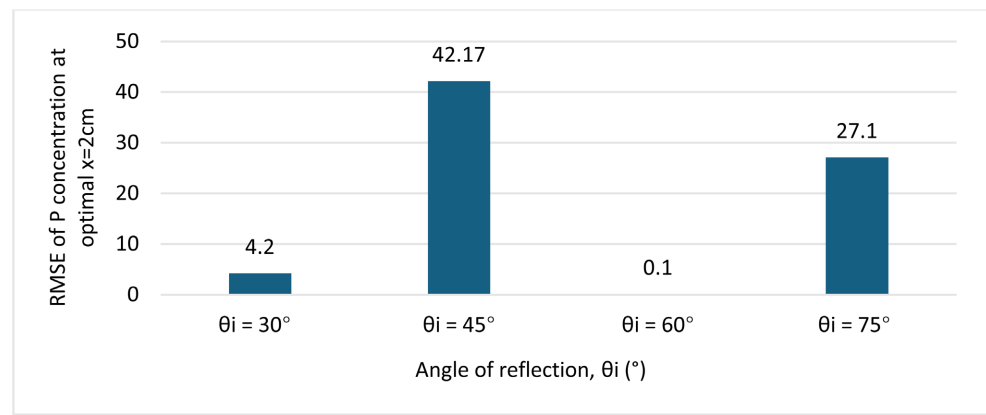
To determine the optimal geometric parameters, root mean square error (RMSE) values were computed for different path lengths and angle of incidence as shown in **Figure 7**. The optimal optical path length and angle of incidence were determined to be 2 cm and 60°, respectively. These optimal parameters provided the most accurate results with the least RMSE, compared to other tested conditions, hence demonstrating their effectiveness in enhancing sensor precision.

As shown in **Figure 6**, the difference in macronutrient concentrations at  $x = 2$  cm compared to the reference concentration was minimal when compared to the differences at  $x = 4$  cm,  $x = 6$  cm,  $x = 8$  cm, and  $x = 10$  cm, making  $x = 2$  cm the optimal value. Hence larger path length resulted in significantly higher RMSE values, and this is primarily due to excessive signal attenuation and scattering effects. Prior studies by Masrie *et al.* [14] and Yusof *et al.* [16], confirm that extended optical path lengths increase light dispersions, adversely affecting nutrient detection. It is therefore essential to select the appropriate optical path length to maintain accuracy and minimize measurement inconsistencies and error.

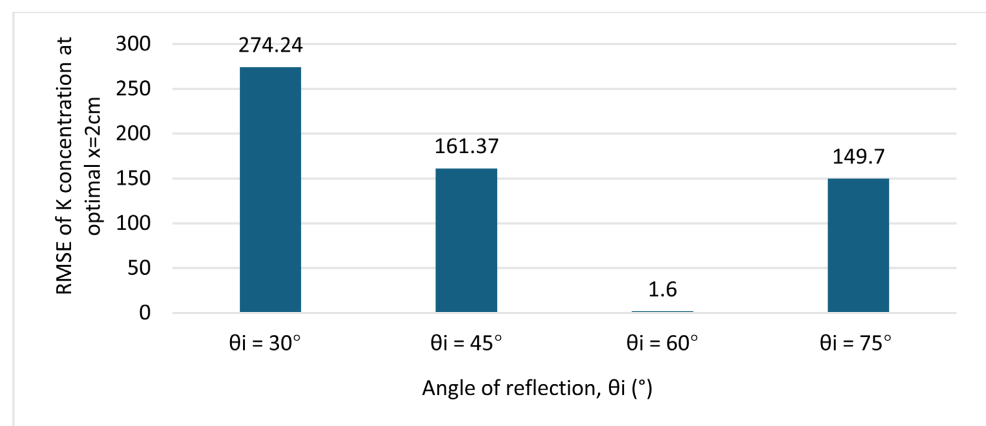
Similarly, an angle of incidence of 60° provided the highest measurement accuracy with a lower RMSE when compared to RMSE values gotten at 30°, 45°, and 75°, as it optimized the balanced between reflected and transmitted light. These findings align with the observations from Ahmed *et al.* [21] and Liu *et al.* [22], who demonstrated that optimizing the angle of incidence leads to enhanced sensor efficiency and reliability. By refining these geometric parameters, optical sensors can be more effectively tailored for agricultural applications, ensuring excellent performance across varying environmental conditions.



(a)



(b)



(c)

**Figure 7.** The RMSE of macronutrient concentration at optimal  $x = 2$  cm. (a) Nitrogen (N); (b) Phosphorus (P); (c) Potassium (K).

### 3.3. Influence of Optimal Geometric Parameters on Sensor Accuracy and Mitigation of External Interference in the Detection of Soil Macronutrient

With the optimal path length and angle of incidence established, further analysis was conducted to assess how these parameters influence sensor accuracy and mit-

igate external interference in detection of soil macronutrients.

It was observed that Phosphorus exhibited a significantly lower RMSE compared to Nitrogen and Potassium. This suggests that the spectral absorption characteristics of Phosphorus aligns more effectively with the emission spectrum of the optical sensor, making its detection less susceptible to geometric variations. The least RMSE for Phosphorus supports findings presented by Kato and Nishimura [23], who demonstrated that phosphorus is more accurately predicted in soil compared to Nitrogen and Potassium. This observation highlights an advantage in Phosphorus detection, indicating that future sensor designs may further need modified calibration methods to maximize accuracy for the detection of Nitrogen and Potassium. Additionally, percentage error calculations performed between experimental macronutrient concentrations at optimal geometric parameters and reference chemical analysis values (shown in **Figure 8**) confirmed minimal errors in Phosphorus detection. This finding is also consistent with studies conducted by Fang *et al.* [24], where sensor geometry optimization was carried out to enhance target localization and nutrient measurement precision.

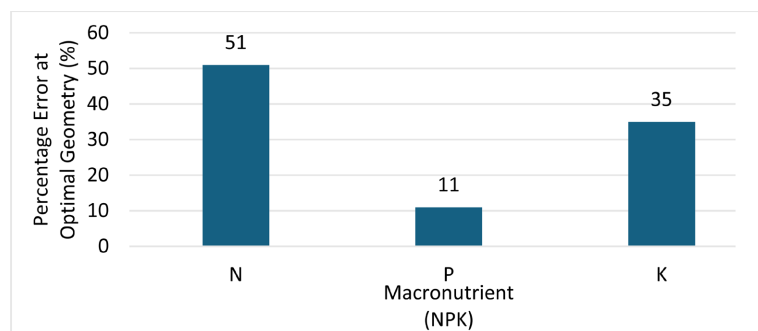


**Figure 8.** The percentage error at optimal geometry.

While the optimal geometric parameters significantly improve sensor accuracy, several challenges must be considered for real-world implementation. First, maintaining precise geometric alignment in field conditions may be difficult due to mechanical disturbances, uneven terrain, or sensor degradation over time [25]. Second, soil composition, texture, and moisture content vary across regions and can influence optical interactions with the sensor. Studies by Kato and Nishimura [23] confirm that changes in soil properties (specifically soil moisture content) significantly affect sensor readings, with dry soil exhibiting lower accuracy compared to wet soil. To address these challenges; calibration models may need to be localized or dynamically adjusted and robust sensor housing and auto-alignment mechanisms may be necessary, along with localized calibration models tailored to regional soil characteristics.

#### 4. Conclusion and Recommendation for Future Work

In this study, we examined the effects of geometric parameters on the response of an optical sensor for detecting soil macronutrients. The primary objective was to

determine the influence of the geometric parameters on the accuracy of the sensor and to determine how these geometric parameters influence the accuracy of the sensor and to identify their optimal values that yield higher accuracy in NPK measurement, comparable to results obtained from chemical analysis. We began by chemically analyzing the experimental sample to determine its exact concentration. Subsequently, considering alignment of sensor elements (photodiode and LEDs) as the key factor of determining the geometric parameters, these parameters were derived using the law of reflection of light. These parameters included the optimal path length ( $x$ ), angles of incidence ( $\theta_i$ ) and reflection ( $\theta_r$ ), and distances between various components ( $d_1$ ,  $d_2$ , and  $D$ ). For all types of optical radiation (infrared, red, and blue), the optimal values for ( $x$ ), ( $D$ ), and ( $\theta_r$ ) were identified as 2 cm, 7 cm, and  $60^\circ$ , respectively. At these dimensions, the sensor error was minimal with a RMSE of 2.1, 0.1, 1.6 for the determination of concentration of Nitrogen, Phosphorus, and Potassium, respectively.

In future research, we plan to conduct a more comprehensive investigation using different types of experimental samples (different soil types) and under different environmental conditions (varying temperature, moisture, etc.), with varying concentrations of nitrogen, phosphorus, and potassium. With these diverse experimental samples, we will examine the sensor's response at the optimal geometric parameters ( $x = 2$  cm,  $D = 7$  cm, and  $\theta_r = 60^\circ$ ) to changes in macronutrient concentrations. This will involve determining how the sensor responds to both increases and decreases in macronutrient concentrations.

## Conflicts of Interest

The authors declare no conflicts of interest regarding the publication of this paper.

## References

- [1] United Nations (2024) World Population Projected to Reach 9.8 Billion in 2050, and 11.2 Billion in 2100. United Nations. <https://www.un.org/en/desa/world-population-projected-reach-98-billion-2050-and-112-billion-2100>
- [2] (2023) Urbanization by Continent 2022. Statista. <https://www.statista.com/statistics/270860/urbanization-by-continent/>
- [3] Beckers, V., Poelmans, L., Van Rompaey, A. and Dendoncker, N. (2020) The Impact of Urbanization on Agricultural Dynamics: A Case Study in Belgium. *Journal of Land Use Science*, **15**, 626-643. <https://doi.org/10.1080/1747423x.2020.1769211>
- [4] Mehta, K., Arora, P., Arora, N. and Aayushi, A. (2022) Enhancement of Smart Agriculture Using Internet of Things. *ECS Transactions*, **107**, Article ID: 7074. <https://doi.org/10.1149/10701.7047ecst>
- [5] Wolfert, S., Ge, L., Verdouw, C. and Bogaardt, M. (2017) Big Data in Smart Farming—A Review. *Agricultural Systems*, **153**, 69-80. <https://doi.org/10.1016/j.agsy.2017.01.023>
- [6] Hossain, M.I., Khaleque, M.A., Ali, M.R., Bacchu, M.S., Hossain, M.S., Shahed, S.M.F., *et al.* (2024) Development of Electrochemical Sensors for Quick Detection of Environmental (Soil and Water) NPK Ions. *RSC Advances*, **14**, 9137-9158.

- <https://doi.org/10.1039/d4ra00034j>
- [7] Laskar, S. and Mukherjee, S. (2016) Optical Sensing Methods for Assessment of Soil Macro-Nutrients and Other Properties for Application in Precision Agriculture: A Review. *Journal of Engineering Technology*, **4**, 206-210.
- [8] Potdar, R.P., Shirolkar, M.M., Verma, A.J., More, P.S. and Kulkarni, A. (2021) Determination of Soil Nutrients (NPK) Using Optical Methods: A Mini Review. *Journal of Plant Nutrition*, **44**, 1826-1839. <https://doi.org/10.1080/01904167.2021.1884702>
- [9] Ameer, S., Ibrahim, H., Kulsoom, F.N.U., Ameer, G. and Sher, M. (2024) Real-time Detection and Measurements of Nitrogen, Phosphorous & Potassium from Soil Samples: A Comprehensive Review. *Journal of Soils and Sediments*, **24**, 2565-2583. <https://doi.org/10.1007/s11368-024-03827-5>
- [10] Pal, A., Dubey, S.K., Goel, S. and Kalita, P.K. (2024) Portable Sensors in Precision Agriculture: Assessing Advances and Challenges in Soil Nutrient Determination. *TrAC Trends in Analytical Chemistry*, **180**, Article ID: 117981. <https://doi.org/10.1016/j.trac.2024.117981>
- [11] Mukherjee, S. and Laskar, S. (2019) Vis-Nir-Based Optical Sensor System for Estimation of Primary Nutrients in Soil. *Journal of Optics*, **48**, 87-103. <https://doi.org/10.1007/s12596-019-00517-1>
- [12] Lourebam, D., Laskar, S. and Mukherjee, S. (2018) Framework for an Optical Sensor System for Monitoring of Soil Nitrogen and Tailoring Soil pH. *Journal of Optics*, **47**, 180-194.
- [13] Macabiog, R.E.N., Fadchar, N.A. and Cruz, J.C.D. (2020) Soil NPK Levels Characterization Using near Infrared and Artificial Neural Network. 2020 16th *IEEE International Colloquium on Signal Processing & Its Applications (CSPA)*, Langkawi, 28-29 February 2020, 141-145. <https://doi.org/10.1109/cspa48992.2020.9068717>
- [14] Masrie, M., Rosli, A.Z.M., Sam, R., Janin, Z. and Nordin, M.K. (2018) Integrated Optical Sensor for NPK Nutrient of Soil Detection. 2018 *IEEE 5th International Conference on Smart Instrumentation, Measurement and Application (ICSIMA)*, Songkhla, 28-30 November 2018, 1-4. <https://doi.org/10.1109/icsima.2018.8688794>
- [15] Tasneem, N., Hasan, M.A., Akther, S.B. and Khan, M.M. (2021) An Automatic Soil Testing Machine for Accurate Fertilization. 2021 *IEEE World AI IoT Congress (AI-IoT)*, Seattle, 10-13 May 2021, 325-331. <https://doi.org/10.1109/aiiot52608.2021.9454248>
- [16] Mohd Yusof, K., Isaak, S., Che Abd Rashid, N. and Ngajikin, N.H. (2016) NPK Detection Spectroscopy on Non-Agriculture Soil. *Jurnal Teknologi*, **78**, No. 11. <https://doi.org/10.11113/jt.v78.8382>
- [17] G, L., C, R. and P, G. (2020) An Automated Low Cost IoT Based Fertilizer Intimation System for Smart Agriculture. *Sustainable Computing: Informatics and Systems*, **28**, Article ID: 100300. <https://doi.org/10.1016/j.suscom.2019.01.002>
- [18] Sabri, N., Aljunid, S.A., Salim, M.S., Ahmad, R.B. and Kamaruddin, R. (2013) Toward Optical Sensors: Review and Applications. *Journal of Physics: Conference Series*, **423**, Article ID: 012064. <https://doi.org/10.1088/1742-6596/423/1/012064>
- [19] Li, Q., Zhong, R., Yang, C., Zhao, K., Zhang, C. and Li, Y. (2022) Geometric Quality Improvement Method of Optical Remote Sensing Satellite Images Based on Rational Function Model. *Remote Sensing*, **14**, Article 4443. <https://doi.org/10.3390/rs14184443>
- [20] Alem, B., Abedian, A. and Nasrollahi-Nasab, K. (2021) Impact of Sensor Geometric Dimensions and Installation Accuracy on the Results of Instantaneous SHM Based

- on Wave Propagation Using Wafer Active Sensors. *Journal of Aerospace Engineering*, **34**, Article ID: 04020100. [https://doi.org/10.1061/\(asce\)as.1943-5525.0001217](https://doi.org/10.1061/(asce)as.1943-5525.0001217)
- [21] Ahmed, T., Hosain, M.K. and Kouzani, A.Z. (2025) Highly Sensitive SPR Sensor Employing Zinc Selenide, Silver Nanocomposite, and Lead Titanate for the Detection of Cancer Cells. *Microchimica Acta*, **192**, Article No. 203. <https://doi.org/10.1007/s00604-024-06867-3>
- [22] Liu, K., Wang, M., Peng, J., Li, S., Luo, Y. and Zhang, X. (2024) Effect of Angle of Incidence on the Optical-Electrical-Thermal Performance of Photovoltaic Insulated Glass Units. *Renewable Energy*, **226**, Article ID: 120364. <https://doi.org/10.1016/j.renene.2024.120364>
- [23] Kato, C. and Nishimura, T. (2016) Predicting Soil Moisture Condition in Arbitrary Agricultural Lands Using the Digital Soil Map and Soil Physical Properties Database. *Paddy and Water Environment*, **15**, 159-169. <https://doi.org/10.1007/s10333-016-0537-z>
- [24] Fang, X., He, Z., Zhang, S., Li, J. and Shi, R. (2022) Improving Localization Accuracy under Constrained Regions in Wireless Sensor Networks through Geometry Optimization. *Entropy*, **25**, Article 32. <https://doi.org/10.3390/e25010032>
- [25] Fan, Y., Wang, X., Funk, T., Rashid, I., Herman, B., Bompoti, N., *et al.* (2022) A Critical Review for Real-Time Continuous Soil Monitoring: Advantages, Challenges, and Perspectives. *Environmental Science & Technology*, **56**, 13546-13564. <https://doi.org/10.1021/acs.est.2c03562>